

# Barrow holographic dark energy models in $f(Q)$ symmetric teleparallel gravity with Lambert function distribution

M. Koussour<sup>1,\*</sup> S.H. Shekh<sup>2,†</sup> H. Filali<sup>3,‡</sup> and M. Bennai<sup>1,3,§</sup>

<sup>1</sup>Quantum Physics and Magnetism Team, LPMC, Faculty of Science Ben M'sik, Casablanca Hassan II University, Morocco.

<sup>2</sup>Department of Mathematics. S. P. M. Science and Gilani Arts Commerce College, Ghatanji, Dist. Yavatmal, Maharashtra-445301, India.

<sup>3</sup>Lab of High Energy Physics, Modeling and Simulations, Faculty of Science, University Mohammed V-Agdal, Rabat, Morocco.

(Dated: September 2, 2022)

The paper presents Barrow holographic dark energy (infrared cut-off is the Hubble horizon) suggested by Barrow recently (Physics Letters B 808 (2020): 135643) in an anisotropic Bianchi type-I Universe within the framework of  $f(Q)$  symmetric teleparallel gravity, where the non-metricity scalar  $Q$  is responsible for the gravitational interaction. We consider two cases: Interacting and non-interacting models of pressureless dark matter and Barrow holographic dark energy by solving  $f(Q)$  symmetric teleparallel field equations. To find the exact solutions of the field equations, we assume that the time-redshift relation follows a Lambert function distribution as  $t(z) = \frac{mt_0}{l} g(z)$ , where  $g(z) = \text{LambertW} \left[ \frac{l}{m} e^{\frac{l - \ln(1+z)}{m}} \right]$ ,  $m$  and  $l$  are non-negative constants and  $t_0$  represents the age of the Universe. Moreover, we discuss several cosmological parameters such as energy density, equation of state (EoS) and skewness parameters, squared sound speed, and  $(\omega_B - \omega'_B)$  plane. Finally, we found the values of the deceleration parameter (DP) for the Lambert function distribution as  $q_{(z=0)} = -0.45$  and  $q_{(z=-1)} = -1$  which are consistent with recent observational data, i.e. DP evolves with cosmic time from initial deceleration to late-time acceleration.

Astronomical observations from Type Ia supernovae (SNIa), Cosmic Microwave Background (CMB), Large Scale Structures (LSS), and even more recent data from multi-wavelength observations of Blazars or the probing of late-time background expansion using gravitational wave sirens with eLISA have shown that the Universe is directed towards an accelerated expansion [1–6]. To explain the observed acceleration, dark energy (DE) was introduced as an added dark component to general relativity (GR) in the form of the cosmological constant ( $\Lambda$ ) and, with dark matter (DM), comprises most of the content of the Universe at present time. Although being the most stable and consistent with observations, the cosmological constant, which finds its origins in vacuum energy, faces many constraints mainly the fine-tuning and coincidence problems [7]. In face of these challenges, other forms of dynamical DE that rely on added exotic forces or matter were proposed such as quintessence, k-essence, phantom energy, Chaplygin gas, etc [8–11].

Another line of research has taken interest in modified gravity theories (MGT) which were introduced as a set

of modifications to Einstein's general relativity which can describe the accelerated expansion without the need for an added component or exotic matter. Various theories of modified gravity were explored in the literature, mainly  $f(R)$  gravity ( $R$  is the Ricci scalar),  $f(G)$  gravity ( $G$  is the Gauss-Bonnet invariant),  $f(R, T)$  gravity ( $R$  is the Ricci scalar and  $T$  is the trace of the stress-energy tensor), and many extensive scalar-tensor theories [12–18].  $f(Q)$  gravity was introduced as a symmetric teleparallel modification of gravity and has gained much interest in recent studies as it has shown many promising results in terms of compatibility with observational constraints [19–35]. It works as a replacement of geometrical formulations in GR by using a non-metricity scalar  $Q$  as a covariant derivative of the metric tensor. Another alternative theory that proved its worth is Holographic dark energy, a model derived from the holographic principle by Susskind et al. that was introduced to cosmology as a way to probe quantum gravity by assuming that the entropy of the Universe is proportional to its area [36–38]. By implementing Bekenstein-Hawking black hole thermodynamics and quantum field theory, Li [39] introduced a model of dark energy density constrained by entropy bounds. More recently, Barrow proposed a modified version of holographic dark energy by taking into account quantum gravitational effects and fractal features of black holes in the dynamics of black hole en-

\* pr.mouhssine@gmail.com

† da.salim@rediff.com

‡ houda.filali318@gmail.com

§ mdbennai@yahoo.fr

tropy which leads to [40]

$$S_B = \left( \frac{A}{A_0} \right)^{\frac{(2+\Delta)}{2}}, \quad (1)$$

where  $A$  and  $A_0$  represent the standard horizon and Planck area, respectively, and  $\Delta$  is a new exponent introduced by Barrow such as  $0 \leq \Delta \leq 1$ . For  $\Delta = 0$ , we retrieve the standard Bekenstein-Hawking entropy. This new form of holographic dark energy has proven to deliver improved cosmological results compared to its standard counterpart, see [41–45]. Motivated by these attractive results, we explore the effects of Barrow holographic dark energy (BHDE) with Hubble horizon as the IR cut-off in the background of anisotropic Bianchi type-I Universe within the framework of  $f(Q)$  symmetric teleparallel gravity. In reality, the anisotropic Universe is motivated by Planck's recent results [46], which confirmed the existence of anomaly in CMB as a result of quantum fluctuations in the era of cosmic inflation, for more details see [47]. Moreover, we find the exact solutions of the field equations assuming the time-redshift relation follows a Lambert function distribution.

This paper is divided as follows: In Sec. I we introduce the field equations of  $f(Q)$  symmetric teleparallel gravity in the background of anisotropic Bianchi type-I Universe, from which we deduct the continuity equations of pressureless dark matter and BHDE. In Sec. II we establish the solution of the field equations by using cosmological constraints and the Lambert function distribution. Further, we consider two cases of study: Interacting and non-interacting  $f(Q)$  models which we will then compare with different existing models of DE. Moreover in Sec. III, we analyze the behavior of the deceleration parameter. Finally in Sec. IV, we discuss and conclude our results.

## I. METRIC AND FIELD EQUATIONS OF $f(Q)$ SYMMETRIC TELEPARALLEL GRAVITY

In the present work, we consider the anisotropic LRS Bianchi type-I Universe metric in the form

$$ds^2 = -dt^2 + A^2(t)dx^2 + B^2(t)(dy^2 + dz^2), \quad (2)$$

where  $A(t)$  and  $B(t)$  are the metric potentials of the Universe which are the functions only of the cosmic time  $(t)$ . The Bianchi type-I Universe becomes isotropic if  $A(t) = B(t) = a(t)$ .

Now, we present the basic equations of  $f(Q)$  symmetric teleparallel gravity. The non-metricity scalar  $Q$  is defined as [19]

$$Q \equiv -g^{\mu\nu}(L^\beta_{\alpha\mu}L^\alpha_{\nu\beta} - L^\beta_{\alpha\beta}L^\alpha_{\mu\nu}), \quad (3)$$

where the disformation tensor  $L^\beta_{\alpha\gamma}$  is formulated as,

$$L^\beta_{\alpha\gamma} = -\frac{1}{2}g^{\beta\eta}(\nabla_\gamma g_{\alpha\eta} + \nabla_\alpha g_{\eta\gamma} - \nabla_\eta g_{\alpha\gamma}). \quad (4)$$

The non-metricity tensor is defined in the form

$$Q_{\gamma\mu\nu} = \nabla_\gamma g_{\mu\nu}, \quad (5)$$

and trace of the non-metricity tensor is derived as follows

$$Q_\beta = g^{\mu\nu}Q_{\beta\mu\nu} \quad \tilde{Q}_\beta = g^{\mu\nu}Q_{\mu\beta\nu}. \quad (6)$$

In addition, we define the superpotential tensor or nonmetricity conjugate as

$$P^\beta_{\mu\nu} = -\frac{1}{2}L^\beta_{\mu\nu} + \frac{1}{4}(Q^\beta - \tilde{Q}^\beta)g_{\mu\nu} - \frac{1}{4}\delta^\beta_{(\mu}Q_{\nu)}. \quad (7)$$

From the above equation, the trace of the non-metricity tensor can be acquired as

$$Q = -Q_{\beta\mu\nu}P^{\beta\mu\nu}. \quad (8)$$

The field equations of  $f(Q)$  symmetric teleparallel gravity are derived from Hilbert–Einstein variational principle. The modified gravity action is given as

$$S = \int \left[ \frac{1}{2\kappa}f(Q) + L_m \right] d^4x \sqrt{-g}, \quad (9)$$

where  $\kappa = 8\pi G$ ,  $f(Q)$  is an arbitrary function of the non-metricity scalar  $Q$ ,  $g$  is the determinant of the metric tensor  $g_{\mu\nu}$  i.e.  $g = \det(g_{\mu\nu})$  and  $L_m$  is the usual matter Lagrangian density. The energy-momentum tensor  $T_{\mu\nu}$  of matter is defined as

$$T_{\mu\nu} = \frac{-2}{\sqrt{-g}} \frac{\delta(\sqrt{-g}L_m)}{\delta g^{\mu\nu}}. \quad (10)$$

Thus, the field equations of  $f(Q)$  symmetric teleparallel gravity are derived by varying the action  $(S)$  in Eq. (9) with respect to the metric tensor  $g_{\mu\nu}$ ,

$$\frac{2}{\sqrt{-g}} \nabla_\beta \left( f_Q \sqrt{-g} P^\beta_{\mu\nu} \right) - \frac{1}{2} f g_{\mu\nu} + f_Q \left( P_{\mu\beta\alpha} Q^\beta_{\nu}{}^{\beta\alpha} - 2 Q^{\beta\alpha}_{\mu} P_{\beta\alpha\nu} \right) = \kappa \left( T_{\mu\nu} + \bar{T}_{\mu\nu} \right), \quad (11)$$

where  $f_Q = \frac{df}{dQ}$ ,  $\nabla_\beta$  is the covariant derivative,  $T_{\mu\nu}$  and  $\bar{T}_{\mu\nu}$  are the energy-momentum tensors of pressureless dark matter and BHDE, respectively. For simplicity, we use natural units ( $\kappa = 1$ ). In addition, by varying the action with respect to the connection, we obtain

$$\nabla_\mu \nabla_\beta \left( f_Q \sqrt{-g} P^\beta_{\mu\nu} \right) = 0. \quad (12)$$

The corresponding non-metricity scalar for metric (2) can be written as

$$Q = -2 \left( \frac{\dot{B}}{B} \right)^2 - 4 \frac{\dot{A}}{A} \frac{\dot{B}}{B}. \quad (13)$$

The energy-momentum tensors for pressureless dark matter and BHDE are defined as

$$T_{\mu\nu} = \rho_M u_\mu u_\nu = \text{diag} [-1, 0, 0, 0] \rho_M, \quad (14)$$

$$\bar{T}_{\mu\nu} = (p_B + \rho_B) u_\mu u_\nu + p_B g_{\mu\nu} = \text{diag} [-1, \omega_B, (\omega_B + \gamma), (\omega_B + \gamma)] \rho_B, \quad (15)$$

where,  $\rho_B$ ,  $\rho_M$  are energy densities of BHDE and pressureless dark matter, respectively, and  $p_B$  is the pressure of BHDE. Here,  $\omega_B = \frac{p_B}{\rho_B}$  is the equation of state (EoS) parameter of the BHDE and  $\gamma$  is the deviations from EoS parameter along  $y$  and  $z$  directions, known as skewness

parameter.

In a comoving co-ordinate system, field equations of  $f(Q)$  symmetric teleparallel gravity (11), with Eqs. (14) and (15) for the Bianchi-I Universe (2) leads to following equations of motion [28]

$$\frac{f}{2} + f_Q \left[ 4 \frac{\dot{A}}{A} \frac{\dot{B}}{B} + 2 \left( \frac{\dot{B}}{B} \right)^2 \right] = \rho_M + \rho_B, \quad (16)$$

$$\frac{f}{2} - f_Q \left[ -2 \frac{\dot{A}}{A} \frac{\dot{B}}{B} - 2 \frac{\ddot{B}}{B} - 2 \left( \frac{\dot{B}}{B} \right)^2 \right] + 2 \frac{\dot{B}}{B} \dot{Q} f_{QQ} = -\rho_B \omega_B, \quad (17)$$

$$\frac{f}{2} - f_Q \left[ -3 \frac{\dot{A}}{A} \frac{\dot{B}}{B} - \frac{\ddot{A}}{A} - \frac{\ddot{B}}{B} - \left( \frac{\dot{B}}{B} \right)^2 \right] + \left( \frac{\dot{A}}{A} + \frac{\dot{B}}{B} \right) \dot{Q} f_{QQ} = -(\omega_B + \gamma) \rho_B. \quad (18)$$

Here,  $(\dot{\phantom{x}})$  dot represents a derivative with respect to cosmic time ( $t$ ). The field equations above (16)-(18) can be represented in the form of mean Hubble and directional Hubble parameters as

$$\frac{f}{2} - Q f_Q = \rho_M + \rho_B, \quad (19)$$

$$\frac{f}{2} + 2 \frac{\partial}{\partial t} [H_y f_Q] + 6 H f_Q H_y = -\rho_B \omega_B, \quad (20)$$

$$\frac{f}{2} + \frac{\partial}{\partial t} \left[ f_Q (H_x + H_y) \right] + 3 H f_Q (H_x + H_y) = -(\omega_B + \gamma) \rho_B, \quad (21)$$

where, we used  $\frac{\partial}{\partial t} \left( \frac{\dot{A}}{A} \right) = \frac{\ddot{A}}{A} - \left( \frac{\dot{A}}{A} \right)^2$  and  $Q = -2H_y^2 - 4H_xH_y$ . Here,  $H = \frac{\dot{a}}{a} = \frac{1}{3} (H_x + 2H_y)$  is the average Hubble parameter and  $H_x = \frac{\dot{A}}{A}$ ,  $H_y = H_z = \frac{\dot{B}}{B}$  represents the directional Hubble parameters along  $x$ ,  $y$  and  $z$  axes, respectively.

Using Eqs. (19)–(21), we obtain the continuity equation of the pressureless dark matter and BHDE as

$$\dot{\rho}_M + \dot{\rho}_B + 3H [\rho_M + (1 + \omega_B) \rho_B] + 2\gamma H_y \rho_B = 0. \quad (22)$$

where the term  $\gamma H_y \rho_B$  in this equation is due to the consideration of the anisotropic fluid.

## II. LAMBERT FUNCTION DISTRIBUTION AND COSMOLOGICAL SOLUTIONS

The above field equations are impossible to find exact solutions to without adding other constraints, because it is a system consisting of three independent equations with seven unknowns:  $H_x$ ,  $H_y$ ,  $\rho_M$ ,  $\rho_B$ ,  $\omega_B$ ,  $\gamma$  and  $f$ . There are several constraints that are used extensively in the literature such as considering the shear scalar ( $\sigma^2$ ) is proportional to the scalar expansion ( $\theta$ ) i.e.  $\sigma^2 \propto \theta$  which leads to a relationship between directional Hubble parameters

$$H_x = kH_y, \quad (23)$$

where  $k \neq 1$  is an arbitrary real number which plays a major role in making the non-isotropic behavior of the Universe. The physical justification for this condition is imposed on the basis of the observations of the velocity redshift relation for extragalactic sources which propose that the Hubble expansion of the Universe may achieve isotropy when  $\frac{\sigma}{\theta}$  is constant [48]. This condition has been used in many works [17, 28].

In addition, we assume that the time-redshift relation  $t(z)$  takes the form of a Lambert function distribution as follows

$$t(z) = \frac{mt_0}{l} g(z), \quad (24)$$

and

$$g(z) = \text{LambertW} \left[ \frac{l}{m} e^{\frac{l - \ln(1+z)}{m}} \right], \quad (25)$$

where  $m$  and  $l$  are non-negative constants and  $t_0$  represents the age of the Universe. This time-redshift relation in Eq. (24) is motivated by the hybrid expansion

law (HEL) of the scale factor of the Universe, which is a combination of power law and exponential law i.e.  $a(t) = a_0 \left( \frac{t}{t_0} \right)^m e^{l \left( \frac{t}{t_0} - 1 \right)}$  where  $a_0$  represents the present value of scale factor of the Universe. The HEL of the scale factor of the Universe gives the exponential law for  $m = 0$  and the power law for  $l = 0$  [49].

Using the relation between the mean scale factor and redshift of the Universe  $a(t) = (1+z)^{-1}$ , and taking into account that the spatial volume  $V = AB^2$ , we find the directional Hubble parameters as

$$H_x = \frac{3k}{k+2} \left( \frac{m}{t} + \frac{l}{t_0} \right) \text{ \& } H_y = H_z = \frac{3}{k+2} \left( \frac{m}{t} + \frac{l}{t_0} \right). \quad (26)$$

Now, by using the Barrow entropy (1), one can obtain the expression for BHDE energy density as follows

$$\rho_B = CL^{\Delta-2}, \quad (27)$$

where  $C$  is a parameter with dimensions  $[L]^{-2-\Delta}$ ,  $L$  can be regarded as the size of the current Universe such as the Hubble scale and the future event horizon, and  $\Delta$  is a free parameter. It can be seen that the above expression provides the standard holographic dark energy model  $\rho_\Lambda = 3M_p^2 L^{-2}$  at  $\Delta = 0$ , where  $C = 3M_p^2$  and  $c$  the velocity of light equal to unity. In the literature, there are several possible choices for infrared cut-off  $L$  that are found in the above BHDE density expression. In this work, for simplicity we will assume the most common form in the literature is the use of Hubble horizon, which is given as

$$\rho_B = CH^{2-\Delta}. \quad (28)$$

By using (26), the Hubble parameter ( $H$ ) for our cosmological model can be obtained in the form

$$H = \frac{1}{3} (H_x + 2H_y) = \frac{m}{t} + \frac{l}{t_0}. \quad (29)$$

Using the above Eqs (28) and (29), we get the energy density of the BHDE as

$$\rho_B = C \left[ \frac{m}{t} + \frac{l}{t_0} \right]^{2-\Delta}. \quad (30)$$

Now, using Eqs. (23) and (26), we get the non-metricity scalar in terms of Hubble parameter of this model as

$$Q = \frac{-18(1+2k)}{(k+2)^2} H^2. \quad (31)$$



We consider the following functional form [29, 50] for our analysis, which is a combination of a linear and a non-linear term of non-metricity scalar  $Q$ ,

$$f(Q) = \alpha Q + \beta Q^n. \quad (32)$$

where  $\alpha$ ,  $\beta$  and  $n \neq 1$  are free model parameters. Capozziello et al. [57] found the best approximation for describing the accelerated expansion of the Universe in  $f(Q)$  gravity is represented by a scenario with  $f(Q) = \alpha + \beta Q^n$ . Using Eqs. (28), (31), (32) in (19), and for this particular  $f(Q)$  cosmological model in Eq. (32), we get the energy density of the pressureless dark matter in terms of Hubble parameter as

$$\rho_M = \frac{9\alpha(1+2k)}{(k+2)^2} H^2 + \frac{(-18)^n \beta (1-2n)(1+2k)^n}{2(k+2)^{2n}} H^{2n} - CH^{2-\Delta}. \quad (33)$$

Using Eqs. (19), (20), (28), (31), (32) in (21) we get the skewness parameter as

$$\gamma = \frac{\gamma_1 (\dot{H} + 3H^2)}{H^{2-\Delta}} + \gamma_2 \left[ (2n-1) \frac{\dot{H}}{H^2} + 3 \right] \frac{H^{2n}}{H^{2-\Delta}}, \quad (34)$$

where

$$\gamma_1 = \frac{3\alpha(1-k)}{C(k+2)}, \quad (35)$$

and

$$\gamma_2 = \frac{3\beta n (-18)^{n-1} (1-k)(1+2k)^{n-1}}{C(k+2)^{2n-1}}. \quad (36)$$

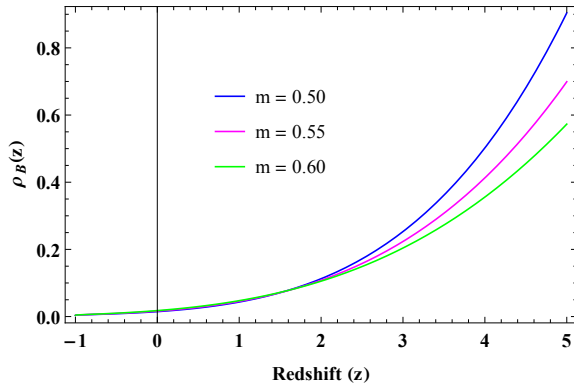


FIG. 1. Plot of energy density ( $\rho_B$ ) of BHDE vs. redshift ( $z$ ) for  $\alpha = 1$ ,  $\beta = -1$ ,  $n = C = 2$ ,  $\Delta = 0.2$ ,  $l = 0.4$ , and  $t_0 = 13.8$ .

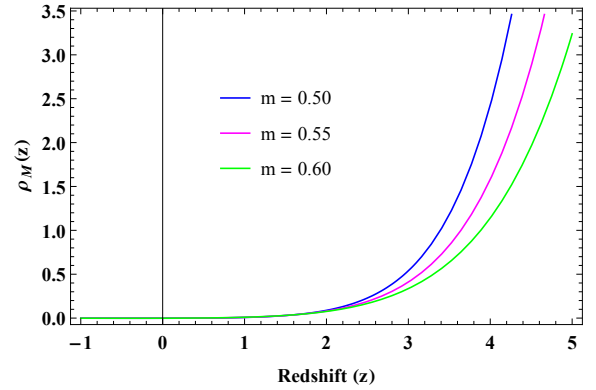


FIG. 2. Plot of energy density ( $\rho_M$ ) of matter vs. redshift ( $z$ ) for  $\alpha = 1$ ,  $\beta = -1$ ,  $n = C = 2$ ,  $\Delta = 0.2$ ,  $l = 0.4$ , and  $t_0 = 13.8$ .

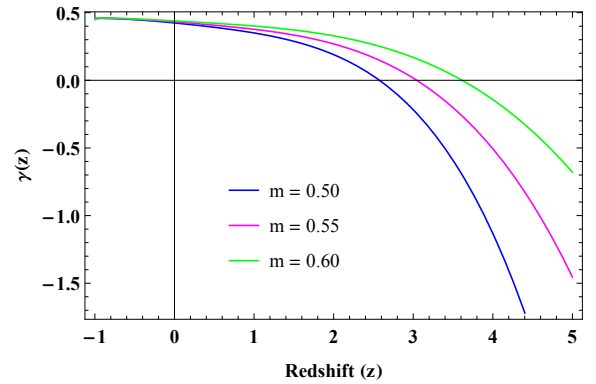


FIG. 3. Plot of skewness parameter ( $\gamma$ ) vs. redshift ( $z$ ) for  $\alpha = 1$ ,  $\beta = -1$ ,  $n = C = 2$ ,  $\Delta = 0.2$ ,  $l = 0.4$ , and  $t_0 = 13.8$ .

In Figs. 1 and 2 we have plotted the behaviors of pressureless dark matter density ( $\rho_M$ ) and BHDE density ( $\rho_B$ ) with the Hubble horizon cut-off in terms of redshift ( $z$ ) for the three different values of  $m = 0.50, 0.55, 0.60$ , respectively. We can see that both  $\rho_M$  and  $\rho_B$  are increasing functions with redshift and positive for all  $z$  values.

Moreover, Fig. 3 represents the behavior of skewness parameter ( $\gamma$ ) in terms of redshift ( $z$ ) for the three different values of  $m$ . From the figure, it is clear that  $\gamma$  is positive at the initial time, and negative at the present i.e.  $z \rightarrow 0$  and future i.e.  $z \rightarrow -1$ . Hence, the BHDE  $f(Q)$  model is anisotropic throughout evolution of the Universe. In the following sections, we will discuss two cases: Non-interacting and interacting  $f(Q)$  model. In addition, we compare these two cases with models of DE in the literature such as the quintessence, phantom,  $\Lambda$ CDM, etc.

#### A. Phantom like behavior of $f(Q)$ non-interacting model

In this subsection, we consider that there is no energy exchange between the two basic components of the Universe: the pressureless dark matter component and BHDE component. Therefore, the continuity equation (22) can be written as

$$\dot{\rho}_M + 3H\rho_M = 0. \quad (37)$$

$$\dot{\rho}_B + 3H(1 + \omega_B)\rho_B + 2\gamma H_y \rho_B = 0. \quad (38)$$

Using Eqs. (28) and (34) in Eq. (38), we get the EoS parameter of BHDE as

$$\omega_B = -1 - \left[ \frac{(2-\Delta)}{3} \frac{\dot{H}}{H^2} + \frac{2\gamma}{(k+2)} \right]. \quad (39)$$

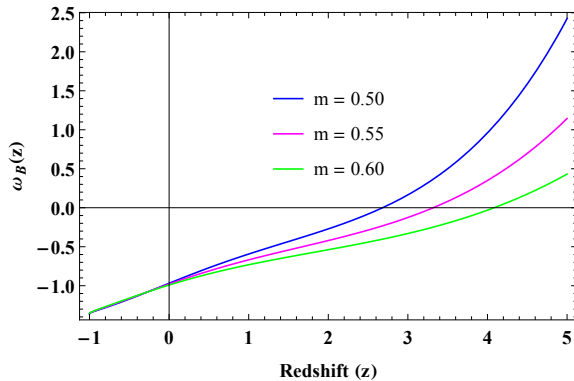


FIG. 4. Plot of EoS parameter ( $\omega_B$ ) vs. redshift ( $z$ ) for  $\alpha = 1$ ,  $\beta = -1$ ,  $n = C = 2$ ,  $\Delta = 0.2$ ,  $l = 0.4$ , and  $t_0 = 13.8$ .

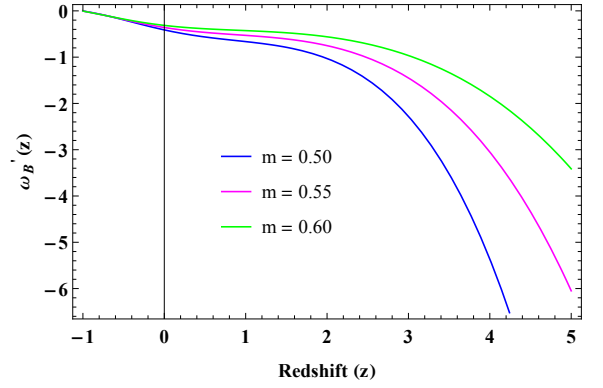


FIG. 5. Plot of  $\omega'_B$  vs. redshift ( $z$ ) for  $\alpha = 1$ ,  $\beta = -1$ ,  $n = C = 2$ ,  $\Delta = 0.2$ ,  $l = 0.4$ , and  $t_0 = 13.8$ .

In this work [51] Caldwell and Linder separate the quintessence phase of DE into two different regions: thawing ( $\omega'_B > 0$ ,  $\omega_B < 0$ ) and freezing ( $\omega'_B < 0$ ,  $\omega_B < 0$ ) regions by introducing a new analysis called  $\omega_B - \omega'_B$  plane. For  $\omega'_B$  prime designate the derivative of EoS parameter with respect to  $x = \ln a$ . Using Eq. (39), we get

$$\omega'_B = \frac{1}{H} \left[ \frac{(2-\Delta)}{3} \left\{ 2 \frac{\dot{H}^2}{H^3} - \frac{\ddot{H}}{H^2} \right\} - \frac{2\dot{\gamma}}{(k+2)} \right], \quad (40)$$

$$\text{where } \dot{\gamma} = H^{\Delta-5} \left[ \begin{aligned} &\gamma_2(2n-1)H^{2n+1}\ddot{H} \\ &+ \gamma_1 H^3 \ddot{H} + \gamma_2(2n-1)(\Delta+2n-4) \\ &\quad \times H^{2n} \dot{H}^2 \\ &+ 3\gamma_2(\Delta+2n-2)H^{2n+2}\dot{H} + \\ &3\gamma_1 \Delta H^4 \dot{H} + \gamma_1(\Delta-2)H^2 \dot{H}^2 \end{aligned} \right],$$

$\dot{H} = -\frac{m}{t^2}$  and  $\ddot{H} = \frac{2m}{t^3}$ . In this background, the squared sound speed ( $v_s^2$ ) is exploited for examining the stability of the dark energy models which is explicit as  $v_s^2 = \frac{dp_B}{d\rho_B} = \frac{\dot{p}_B}{\dot{\rho}_B}$ . If  $v_s^2 > 0$ , we obtain a stable model and if  $v_s^2 < 0$ , we obtain unstable model. For our non-interacting BHDE  $f(Q)$  model  $v_s^2$  takes the following form

$$v_s^2 = -1 + \frac{1}{3} \left[ \left\{ -\frac{(2-\Delta)\dot{H}}{H^2} - \frac{6\gamma}{(k+2)} \right\} + \frac{H}{(2-\Delta)\dot{H}} \right] \quad (41)$$

$$\times \frac{1}{3} \left[ \left\{ -\frac{(2-\Delta)\ddot{H}}{H^2} + \frac{2(2-\Delta)\dot{H}^2}{H^3} - \frac{6\dot{\gamma}}{(k+2)} \right\} \right].$$

In Fig. 4 we plot the behavior of the EoS parameter ( $\omega_B$ ) of non-interacting BHDE  $f(Q)$  model in terms of

redshift ( $z$ ) for three different values of  $m = 0.50, 0.55, 0.60$ . These results can be interpreted as follows: At the beginning of time, the EoS parameter starts from the matter-dominated era, then it moves to the quintessence region ( $-1 < \omega_B < -0.33$ ) and crosses the  $\Lambda$ CDM model ( $\omega_B = -1$ ) in the current time and finally approaches to a phantom region ( $\omega_B < -1$ ). Further, the current values of the EoS parameter are  $\omega_B \sim -1$  ( $z = 0$ ) for the three values of  $m$ . Thus, these values are consistent with Planck 2018 data [52]. The  $\omega'_B$  parameter for non-interacting BHDE  $f(Q)$  model for three different values of  $m$  versus redshift ( $z$ ) is plotted in Fig. 5. It is clear from Figs. 4 and 5 that the  $\omega_B - \omega'_B$  plane corresponds to freezing region for three different values of  $m$ . Fig. 6 shows the evolution of the squared sound speed ( $v_s^2$ ) in terms of redshift ( $z$ ). We can see that  $v_s^2$  is positive in the initial time i.e. our model is stable, and negative in the present and future i.e. an unstable model.

### B. $\Lambda$ CDM like behavior of $f(Q)$ interacting model

In this case, we assume that the pressureless dark matter component is interacting with the BHDE component via the interaction term  $Q$ , we can write the continuity equation of pressureless dark matter and BHDE as

$$\dot{\rho}_M + 3H\rho_M = Q. \quad (42)$$

$$\dot{\rho}_B + 3H(1 + \omega_B)\rho_B + 2\gamma H_y \rho_B = -Q. \quad (43)$$

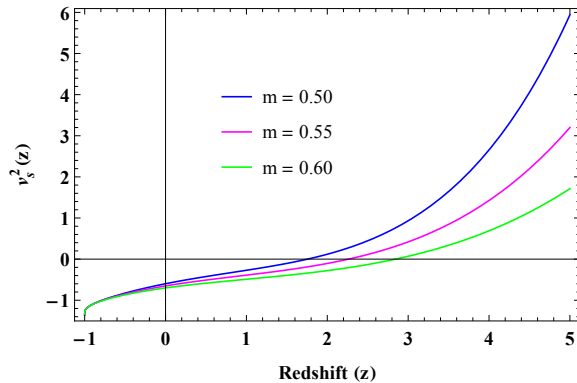


FIG. 6. Plot of squared sound speed ( $v_s^2$ ) vs. redshift ( $z$ ) for  $\alpha = 1, \beta = -1, n = C = 2, \Delta = 0.2, l = 0.4$ , and  $t_0 = 13.8$ .

From the above continuity equation, we can see that the interaction term must be proportional to a quantity with units of inverse of cosmic time. Therefore, this term in the literature can take several forms ( $Q$ -classes) such as  $Q = 3\eta H\rho_M$ ,  $Q = 3\eta H\rho_{DE}$ , and  $Q = 3\eta H(\rho_M + \rho_{DE})$  [53–55]. In this study, we choose  $Q = 3\eta H\rho_B$  as an interaction term where  $3\eta H$  is the decay rate with a coupling constant  $\eta$  (interaction parameter) [56]. In general, the interaction parameter  $\eta$  can be positive or negative. If  $\eta$  is positive means BHDE decays to pressureless DM, while if  $\eta$  is negative means pressureless DM decays to BHDE. The previous situation of the non-interacting  $f(Q)$  model can be obtained with  $\eta = 0$ .

Using Eqs. (28) and (34) in (43), we get the EoS parameter for this case as

$$\omega_B = -1 - \eta - \left[ \frac{(2 - \Delta)}{3} \frac{\dot{H}}{H^2} + \frac{2\gamma}{(k + 2)} \right]. \quad (44)$$

Using the same method in the previous case, we find the derivative of  $\omega_B$  with respect to  $x = \ln a$  as follows

$$\omega'_B = \frac{1}{H} \left[ \frac{(2 - \Delta)}{3} \left\{ 2 \frac{\dot{H}^2}{H^3} - \frac{\ddot{H}}{H^2} \right\} - \frac{2\dot{\gamma}}{(k + 2)} \right]. \quad (45)$$

The squared sound speed ( $v_s^2$ ) in this case is derived as

$$v_s^2 = -1 - \eta + \frac{1}{3} \left[ \frac{(\Delta - 2)\dot{H}}{H^2} - \frac{H}{(\Delta - 2)\dot{H}} \left\{ \frac{(\Delta - 2)\ddot{H}}{H^2} - \frac{2(\Delta - 2)\dot{H}^2}{H^3} - \frac{6\dot{\gamma}}{(k + 2)} \right\} - \frac{6\gamma}{(k + 2)} \right]. \quad (46)$$

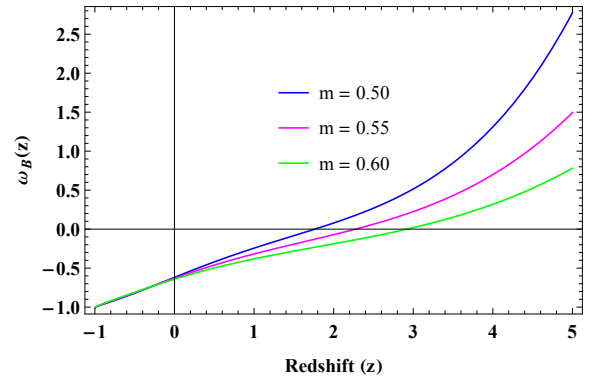


FIG. 7. Plot of EoS parameter ( $\omega_B$ ) vs. redshift ( $z$ ) for  $\alpha = 1, \beta = -1, n = C = 2, \Delta = 0.2, l = 0.4, t_0 = 13.8$  and  $\eta = -0.35$ .

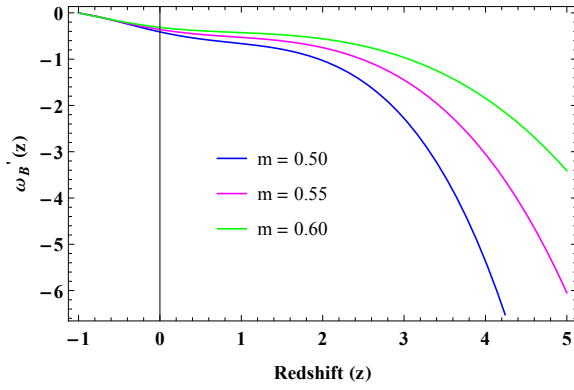


FIG. 8. Plot of  $\omega'_B$  vs. redshift ( $z$ ) for  $\alpha = 1, \beta = -1, n = C = 2, \Delta = 0.2, l = 0.4, t_0 = 13.8$  and  $\eta = -0.35$ .

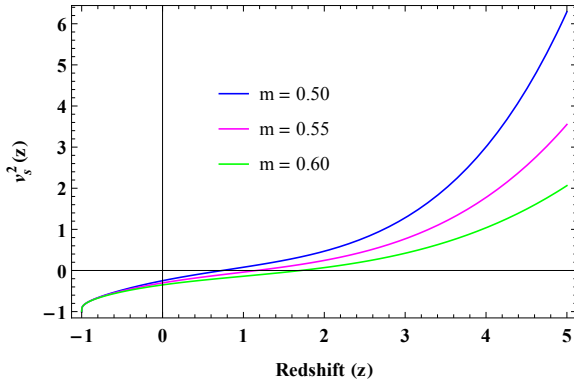


FIG. 9. Plot of squared sound speed ( $v_s^2$ ) vs. redshift ( $z$ ) for  $\alpha = 1, \beta = -1, n = C = 2, \Delta = 0.2, l = 0.4, t_0 = 13.8$  and  $\eta = -0.35$ .

Fig. 7 describes the behavior of EoS parameter ( $\omega_B$ ) for interacting BHDE  $f(Q)$  model in terms of redshift ( $z$ ) for three different values of  $m$ . We also observe that the model begins from a matter-dominated era, varies in the quintessence region, and finally approaches to standard  $\Lambda$ CDM model. Further, the current value of  $\omega_B$  corresponds to the most recent data. The  $\omega'_B$  parameter for interacting BHDE  $f(Q)$  model versus redshift ( $z$ ) for three different values of  $m$  is plotted in Fig. 8. It is clear that the  $\omega_B - \omega'_B$  plane corresponds to freezing region for three different values of  $m$ . Fig. 9 shows the evolution of the squared sound speed ( $v_s^2$ ) versus redshift ( $z$ ). It can be observed that  $v_s^2$  of interacting BHDE  $f(Q)$  model is positive in the initial time i.e. the model is stable, and negative in the present and future i.e. we get an unstable model.

### III. DECELERATION PARAMETER

To verify that the proposed model predicts an accelerating phase of the Universe, we study the behavior of the deceleration parameter (DP) of our cosmological models. The DP sign indicates if the model is accelerating or decelerating. If  $q > 0$ , the model with a deceleration expansion, if  $q = 0$  a constant rate of expansion and an accelerated expansion if  $q < 0$ . The DP for our cosmological models is given by

$$q = -1 + \frac{d}{dt} \left( \frac{1}{H} \right) = -1 + mt_0^2 (mt_0 + lt)^{-2} \quad (47)$$

The behavior of DP ( $q$ ) in terms of redshift ( $z$ ) is shown in Fig. 10. It can be seen that the DP for our models evolves with cosmic time from initial deceleration with positive values to late-time acceleration with negative values and finally approaches to  $-1$ . Further, the current values  $q_0$  ( $z = 0$ ) of the DP correspond to the observational data of SNeIa and CMBR.

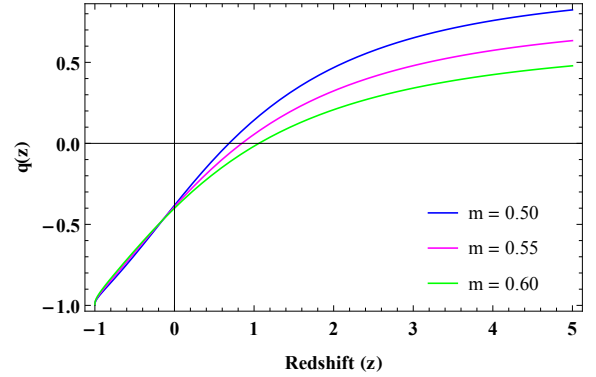


FIG. 10. Plot of deceleration parameter  $q$  vs. redshift  $z$  for  $\alpha = 1, \beta = -1, n = C = 2, \Delta = 0.2, l = 0.4, t_0 = 13.8$  and  $\eta = -0.35$ .

### IV. CONCLUSIONS

In this paper, we have investigated the Barrow holographic dark energy in an anisotropic Bianchi type-I Universe within the framework of  $f(Q)$  symmetric teleparallel gravity, where the non-metricity scalar  $Q$  is responsible for the gravitational interaction. To discuss the current cosmic acceleration, we considered two cases for the study: Interacting and non-interacting models of pressureless dark matter and BHDE. Then we used two main hypotheses in this work: (i) we assumed that the shear scalar ( $\sigma^2$ ) is proportional to the scalar expansion ( $\theta$ ) i.e.  $\sigma^2 \propto \theta$  which leads to a relationship

between directional Hubble parameters as  $H_x = kH_y$ , where  $k \neq 0, 1$ , (ii) we assumed that the redshift-time relation follows the form of a Lambert function distribution. In addition, we considered the  $f(Q)$  model as a combination of a linear and a non-linear term of non-metricity scalar  $Q$  i.e.  $f(Q) = \alpha Q + \beta Q^n$ , where  $\alpha$ ,  $\beta$  and  $n \neq 1$  are free model parameters. We have discussed the behavior of various cosmological parameters that are used in this context, and the following are the most important results obtained: We observed for our models that both pressureless dark matter density and BHDE density are increasing functions with redshift and positive for all  $z$  values (Figs. 1 and 2). Further, we observed that the skewness parameter is positive at the initial time and negative at the present and future (Fig. 3). Hence, the BHDE  $f(Q)$  model is anisotropic throughout evolution of the Universe.

Another interesting result of our cosmological models is that the EoS parameter of non-interacting BHDE  $f(Q)$  model is similar to phantom model and interacting BHDE  $f(Q)$  model like  $\Lambda$ CDM (Figs. 4 and 7). The

evolution of the  $\omega_B - \omega'_B$  plane for both models: Non-interacting and interacting BHDE  $f(Q)$  models corresponds to freezing region ( $\omega'_B < 0, \omega_B < 0$ ) for three different values of  $m$ . Furthermore, we investigated the behavior of squared sound speed for both models. We also found that both models are stable at the beginning of time and unstable at the present and future periods. Finally, the evolution of the deceleration parameter in Fig. 10 indicates a transition of the Universe from decelerated to accelerated phase. Further, we found the values of the deceleration parameter (DP) for the Lambert function distribution as  $q_{(z=0)} = -0.45$  and  $q_{(z=-1)} = -1$  which are consistent with recent observational data.

## ACKNOWLEDGMENTS

We are very much grateful to the honorary referee and the editor for the illuminating suggestions that have significantly improved our work in terms of research quality and presentation.

- 
- [1] A. G. Riess et al., Observational evidence from supernovae for an accelerating Universe and a cosmological constant, *The Astronomical Journal* **116** (1998) 1009.
  - [2] A. G. Riess et al., Type Ia supernova discoveries at  $z > 1$  from the Hubble Space Telescope: Evidence for past deceleration and constraints on dark energy evolution. *The Astrophysical Journal* **607** (2004) 665.
  - [3] S. Hanany et al., MAXIMA-1: a measurement of the cosmic microwave background anisotropy on angular scales of  $10'-5$ , *The Astrophysical Journal* **545** (2000) L5.
  - [4] A. Domínguez and P. Francisco, Measurement of the Expansion Rate of the Universe from U3b3-Ray Attenuation, *The Astrophysical Journal Letters* **771** (2013) L34.
  - [5] D. J. Eisenstein et al., Detection of the baryon acoustic peak in the large-scale correlation function of SDSS luminous red galaxies. *The Astrophysical Journal* **633** (2005) 560.
  - [6] N. Tamanini et al., Science with the space-based interferometer eLISA. III: Probing the expansion of the Universe using gravitational wave standard sirens, *Journal of Cosmology and Astroparticle Physics*. **04** (2016) 002.
  - [7] C. Armendariz-Picon, V. Mukhanov, and S. J. Paul, Dynamical solution to the problem of a small cosmological constant and late-time cosmic acceleration, *Physical Review Letters* **85** (2000) 4438.
  - [8] I. Zlatev, W. Limin, and J. S. Paul, Quintessence, cosmic coincidence, and the cosmological constant, *Physical Review Letters* **82** (1999) 896.
  - [9] P. Armendariz, V. M. Christian, Mukhanov, and J. S. Paul. Essentials of k-essence, *Physical Review D* **63** (2001) 103510.
  - [10] H. Štefančič, Generalized phantom energy. *Physics Letters B* **586** (2004) 5-10.
  - [11] N. Bilić, B. Gary. Tupper, and R. D. Viollier. Unification of dark matter and dark energy: the inhomogeneous Chaplygin gas. *Physics Letters B* **535** (2002) 17-21.
  - [12] S. Nojiri and S. D. Odintsov. Unified cosmic history in modified gravity: from  $F(R)$  theory to Lorentz non-invariant models. *Physics Reports* **505** (2011) 59-144.
  - [13] S. Nojiri and D. Sergei. Introduction to modified gravity and gravitational alternative for dark energy. *International Journal of Geometric Methods in Modern Physics* **4** (2007) 115-145.
  - [14] T. Harko et al.  $f(R, T)$  gravity. *Physical Review D* **84** (2011) 024020.
  - [15] M. Koussour, and M. Bennai. On a Bianchi type-I space-time with bulk viscosity in  $f(R, T)$  gravity. *International Journal of Geometric Methods in Modern Physics* (2021): 2250038.
  - [16] M. Koussour, and M. Bennai. Cosmological models with cubically varying deceleration parameter in  $f(R, T)$  gravity. *Afrika Matematika* **33** (2022) 1-16.
  - [17] M. Koussour et al. Holographic dark energy in Gauss-Bonnet gravity with Granda-Oliveros cut-off. *Nuclear Physics B* (2022): 115738.
  - [18] M. Koussour and M. Bennai. Stability analysis of anisotropic Bianchi type-I cosmological model in telepar-



- allel gravity. *Classical and Quantum Gravity* **39** (2022) 105001.
- [19] J. Jiménez, H. Lavinia and K. Tomi, Coincident general relativity. *Physical Review D* **98** (2018) 044048.
- [20] S. Mandal, P. K. Sahoo, and J. R. L. Santos. *Energy conditions in  $f(Q)$  gravity*. *Physical Review D* **102** (2020) 024057.
- [21] S. Mandal, D. Wang, and P. K. Sahoo. Cosmography in  $f(Q)$  gravity. *Physical Review D* **102** (2020) 124029.
- [22] R. H. Ling and X. H. Zhai. Spherically symmetric configuration in  $f(Q)$  gravity. *Physical Review D* **103** (2021) 124001.
- [23] N. Frusciante, Signatures of  $f(Q)$  gravity in cosmology. *Physical Review D* **103** (2021) 044021.
- [24] W. Khyllep, P. Andronikos and J. Dutta. Cosmological solutions and growth index of matter perturbations in  $f(Q)$  gravity. *Physical Review D* **103** (2021) 103521.
- [25] T. Harko et al., Coupling matter in modified  $Q$  gravity. *Physical Review D* **98** (2018) 084043.
- [26] N. Dimakis, A. Paliathanasis, and T. Christodoulakis. Quantum cosmology in  $f(Q)$  theory. *Classical and Quantum Gravity* **38** (2021) 225003.
- [27] B. Jing, T. H. Loo, and A. De. Geodesic deviation equation in  $f(Q)$  gravity. *Chinese Journal of Physics* (2021).
- [28] De, Avik, et al. Isotropization of locally rotationally symmetric Bianchi-I Universe in  $f(Q)$  gravity. *The European Physical Journal C* **82** (2022) 1-11.
- [29] S. H. Shekh, Models of holographic dark energy in  $f(Q)$  gravity. *Physics of the Dark Universe* **33** (2021) 100850.
- [30] M. Koussour, S. H. Shekh, and M. Bennai. Cosmic acceleration and energy conditions in symmetric teleparallel  $f(Q)$  gravity. *Journal of High Energy Astrophysics* **35** (2022) 43-51.
- [31] M. Koussour et al. Flat FLRW Universe in logarithmic symmetric teleparallel gravity with observational constraints. *Classical and Quantum Gravity* doi: 10.1088/1361-6382/ac8c7d (2022).
- [32] M. Koussour, S. H. Shekh, and M. Bennai. Anisotropic nature of space-time in  $f(Q)$  gravity. *Physics of the Dark Universe* (2022): 101051.
- [33] M. Koussour et al. Thermodynamical aspects of Bianchi type-I Universe in quadratic form of  $f(Q)$  gravity. *arXiv preprint arXiv:2203.03639* (2022).
- [34] M. Koussour, S. H. Shekh, and M. Bennai. Bianchi type-I Barrow holographic dark energy model in symmetric teleparallel gravity. *arXiv preprint arXiv:2203.08181* (2022).
- [35] M. Koussour, S. H. Shekh, and M. Bennai. Anisotropic  $f(Q)$  gravity model with bulk viscosity. *arXiv preprint arXiv:2203.10954* (2022).
- [36] G. Hooft, Dimensional reduction in quantum gravity. *arXiv preprint gr-qc/9310026* (1993).
- [37] L. Susskind, The world as a hologram. *Journal of Mathematical Physics* **36** (1995) 6377-6396.
- [38] A. Cohen, B. David and A. E. Nelson. Effective field theory, black holes, and the cosmological constant. *Physical Review Letters* **82** (1999) 4971.
- [39] M. Li, A model of holographic dark energy. *Physics Letters B* **603** (2004) 1-5.
- [40] J. Barrow, The area of a rough black hole. *Physics Letters B* **808** (2020) 135643.
- [41] E. N. Saridakis, Barrow holographic dark energy. *Physical Review D* **102** (2020) 123525.
- [42] A. K. nagnostopoulos, S. Basilakos, and E. N. Saridakis. Observational constraints on Barrow holographic dark energy. *The European Physical Journal C* **80** (2020) 1-9.
- [43] A. Priyanka, et al. Barrow holographic dark energy in a nonflat Universe. *Physical Review D* **104** (2021) 123519.
- [44] S. Srivastava and U. K. Sharma. Barrow holographic dark energy with Hubble horizon as IR cutoff. *International Journal of Geometric Methods in Modern Physics* **18** (2021): 2150014.
- [45] U. K. Sharma, V. G. Varshney, and V. C. Dubey. Barrow agegraphic dark energy. *International Journal of Modern Physics D* **30** (2021) 2150021.
- [46] P. A. R. Ade et al. Planck 2015 results-XVI. Isotropy and statistics of the CMB. *Astronomy & Astrophysics* **594** (2016) A16.
- [47] P. K. Sahoo, P. Sahoo, and B. K. Bishi. Anisotropic cosmological models in  $f(R, T)$  gravity with variable deceleration parameter. *International Journal of Geometric Methods in Modern Physics* **14** (2017) 1750097.
- [48] C. B. Collins and S. W. Hawking. Why is the Universe isotropic?. *The Astrophysical Journal* **180** (1973) 317-334.
- [49] O. Akarsu, et al. Cosmology with hybrid expansion law: scalar field reconstruction of cosmic history and observational constraints. *Journal of Cosmology and Astroparticle Physics* **01** (2014) 022.
- [50] R. Solanki, Avik De, and P. K. Sahoo. Complete dark energy scenario in  $f(Q)$  gravity. *Physics of the Dark Universe* (2022) 100996.
- [51] R. R. Caldwell, and E. V. Linder. Limits of quintessence. *Physical review letters* **95** (2005) 141301.
- [52] A. Nabila et al. Planck 2018 results-VI. Cosmological parameters. *Astronomy & Astrophysics* **641** (2020) A6.
- [53] J. He and B. Wang. Effects of the interaction between dark energy and dark matter on cosmological parameters. *Journal of Cosmology and Astroparticle Physics* **06** (2008) 010.
- [54] M. V. Santhi, and Y. Sobhanbabu. Bianchi type-III Tsallis holographic dark energy model in Saez-Ballester theory of gravitation. *The European Physical Journal C* **80** (2020) 1-15.
- [55] B. Wang et al. Interacting dark energy and dark matter: observational constraints from cosmological parameters. *Nuclear Physics B* **778** (2007) 69-84.
- [56] S. Sarkar, Interacting holographic dark energy with variable deceleration parameter and tachyon scalar field dark energy model in LRS Bianchi type-II Universe. *Astrophysics and Space Science* **350** (2014) 821-829.
- [57] S. Capozziello and R. D'Agostino. Model-independent reconstruction of  $f(Q)$  non-metric gravity. *Physics Letters B* (2022): 137229.